

Supporting Information

Potential dependence of the ionic structure
at the ionic liquid/water interface
studied using MD simulation

Kosuke Ishii, Tetsuo Sakka, and Naoya Nishi*

Department of Energy and Hydrocarbon Chemistry, Graduate School of Engineering,

Kyoto University, Kyoto 615-8510, Japan.

E-mail: nishi.naoya.7e@kyoto-u.ac.jp

1. Preparation of the IL-W two-phase system in MD

The initial configuration for the bulk MD of IL was created by using the `fftool`¹ and `Packmol`.² The system was optimized in the NPT ensemble at 20 K (2.0 ps, Berendsen thermostat³), followed by sequential equilibration runs at 423 K (1.0 ns, Berendsen thermostat), 700 K (0.5 ns, Berendsen thermostat), 600 K (0.3 ns, Nosé-Hoover thermostat,^{4,5} 500 K (0.3 ns, Nosé-Hoover thermostat), 423 K (1.5 ns, Nosé-Hoover thermostat). A cubic liquid bulk with a length of 51.6 Å was obtained.

The bulk MD of W was similarly performed by sequential equilibration runs at 100 K, 200 K, 300 K (2.0 ps, Berendsen thermostat respectively), 423 K (0.5 ns, Berendsen thermostat), and 423 K (1.5 ns, Nosé-Hoover thermostat). The obtained bulk of W was a cube with a length of 51.2 Å.

The obtained simulation boxes by the bulk MDs of IL and W were combined as follows. The periodic boundary condition in the z-axis direction of the boxes was released in the same way as Katakura et al.⁶ The boxes were then stretched and contracted in the *xy* direction to match the *xy* size of the graphene plate introduced below. Then, the boxes were combined in the z-direction with a thin vacuum layer between them to avoid too strong interatomic repulsive force during the initial equilibration. Two graphene plates (1008 C atoms, 51.69 Å × 51.16 Å in the *xy* plane) were inserted as follows. The first graphene plate was put next to the W box, on the opposite side of the IL|W interface, with the z position about 5 Å away from the closest atom of H₂O on the boundary. Inserting the graphene plate 5 Å away from the W box prevented the graphene from overlapping with the atoms of W. The second plate was put with the z position 80 Å away from the IL box. The two graphene plates were separated by 70 Å across the periodic boundary of the *xy*-plane. Then, the system was equilibrated for 1.0 ns at 423 K (NVT and Berendsen thermostat). The following simulations were performed at 423K with NVT.

The second graphene plate was brought closer to the IL-W system about 10 Å away from the IL boundary on the opposite side of the IL|W interface, followed by 1.0 ns equilibration. Since the IL

ions are much larger than water molecules, the graphene on the IL side was inserted with a wider gap compared with the graphene on the water side. The two graphene plates were separated by 120 Å across the periodic boundary of the xy-plane. Since vacuum gaps were introduced between graphene and W, W and IL, and IL and graphene, the IL and W phases were expanded during the equilibration, and therefore the bulk densities of the IL and W phases in the resulting MD cell were lower than those in the bulk MD. By compressing the entire cell in the z-direction, the densities of IL and W phases (1.13 \AA^{-3} and 0.93 \AA^{-3} respectively) were adjusted to be the same as those in the bulk MD of the IL and W (1.18 \AA^{-3} and 0.91 \AA^{-3} respectively), which was judged by the density distribution after the 0.5 ns equilibration with the Berendsen thermostat. Finally, the size of the simulation cell was $51.7 \times 51.2 \times 250 \text{ \AA}$, with a 140 Å thick vacuum layer on the outside of the graphene/W/IL/graphene sandwich (Fig. 1b).

The MD process for the IL/W interface is shown in Fig. S1. First, an equilibration run was performed for 2.0 ns (1.0 ns each with the Berendsen and Nosé-Hoover thermostats), without putting any charge on the graphene atoms. For the MD with charged conditions, the C atoms of the two graphene plates on the IL and W side were charged ($q_{g,IL} = \pm 6.06, \pm 3.03 \text{ \mu C cm}^{-2}$, $q_{g,W} = -q_{g,IL}$) and equilibrated for 2.0 ns with Nosé-Hoover thermostat. The first production run at each charge was then performed for 10 ns. Then, to perform calculations from different initial configurations, the final configuration of the 10 ns production run at the different potential was used as the initial configuration for the next 10 ns, as shown in Fig.S1d. After 2 ns of equilibration, the second production run of 10 ns was performed. The number density distribution and orientation analysis were performed with the 20 ns run in total.

The MD of the IL|vacuum interface was also performed to compare the interfacial orientation of IL ions. Two IL bulk MD boxes were stacked similarly to our previous MD study on the vacuum interface of ILs,⁶ and a vacuum layer was added so that the z-axis length of the simulation box was

300 Å. The initial configuration of the IL|vacuum interface MD was equilibrated at 423 K and in the NVT ensemble (2.5 ns, Berendsen thermostat), and a production run (10.0 ns, Nosé-Hoover thermostat) were performed.

2. Orientation of H₂O

We analyzed the orientation of the dipole moment of water (defined in Fig.S8) on the W side of the IL|W interface. The dipole moment at $\Delta E = 0$ was preferentially oriented toward the IL side (the black curve in Fig. S9), which means that the H atoms of a water molecule at the interface are relatively located on the IL side than the O atom. Previous studies using VSF^{7,8} and MD⁸ at the CCl₄|W interface, which is not an electrochemical interface, suggested that OH bonds without hydrogen bonding (Free OH) are abundantly distributed at the interface (MD)⁸ and the Free OH bonds direct their H atoms to the CCl₄ phase (VSF).^{7,8} The water orientation in the present study at $\Delta E = 0$ agrees with the previous studies.^{7,8} At $\Delta E > 0$ ($\Delta E < 0$), the dipole moment was oriented toward the W side (IL side), reacting to and screening the potential that originated from the ion distributions on both sides of the IL|W interface, (i.e., in the electric double layer).

To investigate the contribution of water to the polarization of the interface, the charge density distribution of water alone was analyzed (Fig.S3a). In the charge density distribution of water, for $\Delta E \leq 0$ ($\Delta E > 0$), the charge density distribution was negative (positive) on the W side and positive (negative) on the IL side. This indicates that for $\Delta E \leq 0$ ($\Delta E > 0$), the O atoms of water exist on the W (IL) side and the H atoms on the IL (W) side, which is consistent with the results of orientation analysis. For $\Delta E \leq 0$ on the IL side, the charge density of water was positive enough to outstrip the negative total ionic charge, and the overall charge density distribution was positive (Fig.S3b). This suggests that water has a significant effect on the interfacial polarization.

3. SI Figures and tables

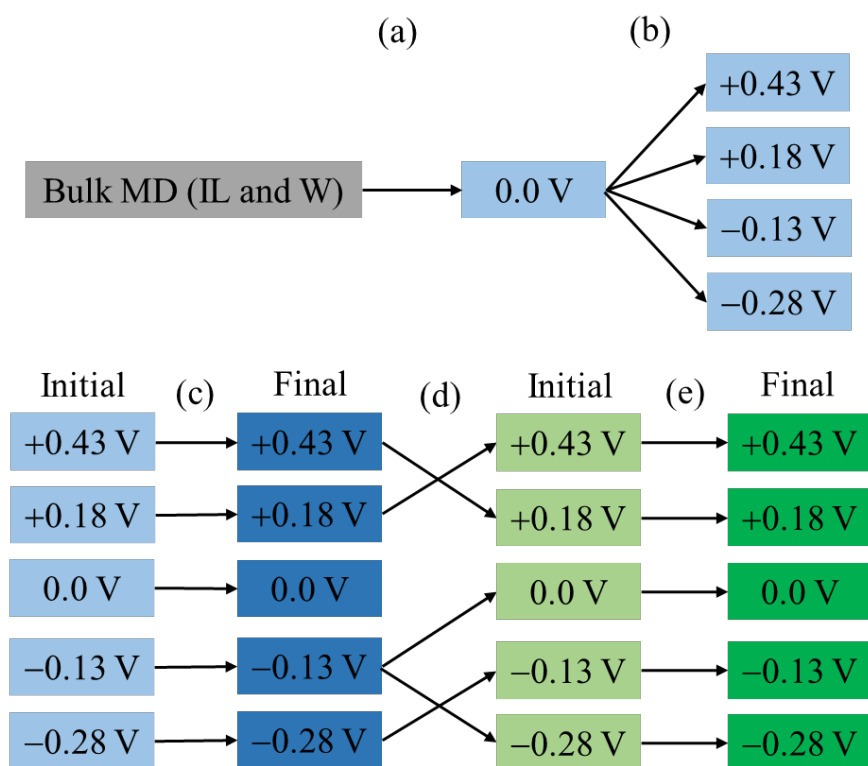


Fig.S1. Flowchart of MD. (a) The bulk MD boxes of W and IL were combined and then sandwiched with two graphene plates, whose location was finally adjusted so that the IL and W densities become those in the bulk MD. 2.0 ns equilibration followed. (b) Charge was put to the graphene C atoms to apply the interfacial potential difference, followed by 2.0 ns equilibration. (c) First 10 ns simulation. (d) The interfacial potential difference was changed as shown by the arrows, followed by 2.0 ns equilibration. (e) Second 10 ns simulation.

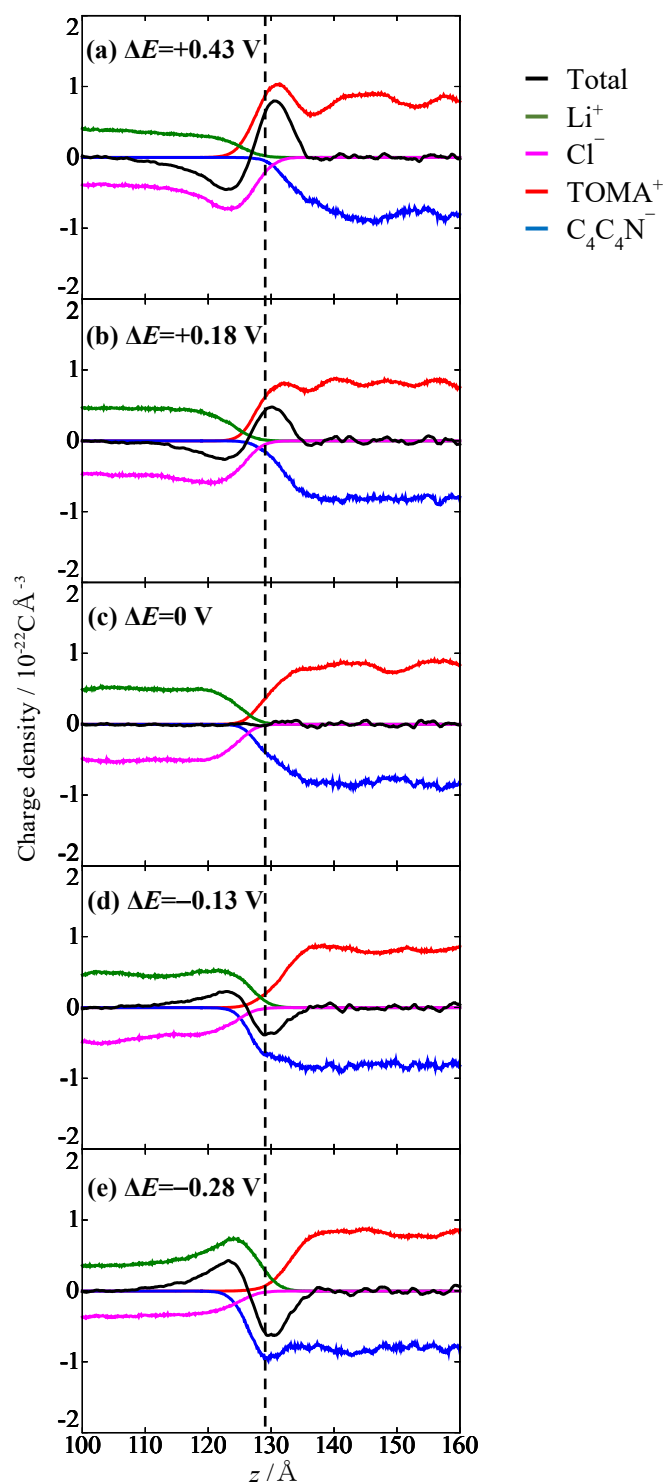


Fig.S2. Charge density profiles at the IL|W for the total ionic charge (black) and the charge of TOMA^+ (red), $\text{C}_4\text{C}_4\text{N}^-$ (dark blue), Li^+ (dark green), and Cl^- (pink) at (a) $\Delta E = +0.43$, (b) $+0.18$, (c) 0 , (d) -0.13 , and (e) -0.28 V . The vertical dotted lines in (a-e) represent the position of the IL|W interface.

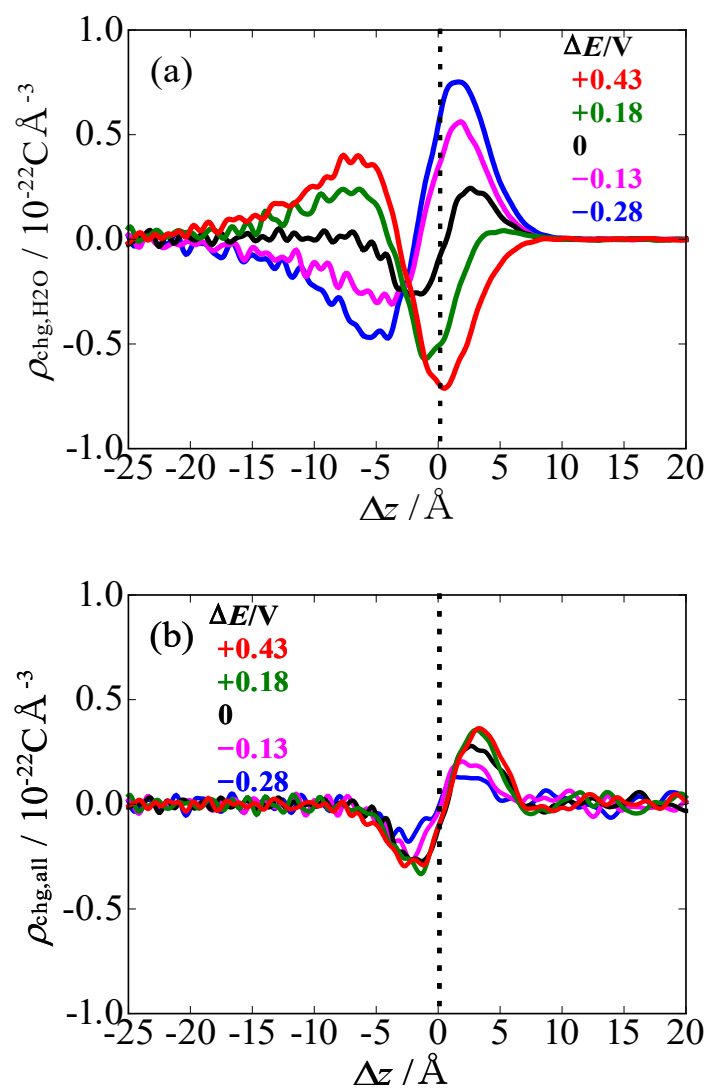


Fig.S3. Charge density distribution for H_2O (a) and all charges (b) at the IL|W interface at $\Delta E=+0.43$ (red), $+0.18$ (dark green), 0 (black), -0.13 (pink) and -0.28 V (blue). The vertical dotted lines represent the position of the IL|W interface.

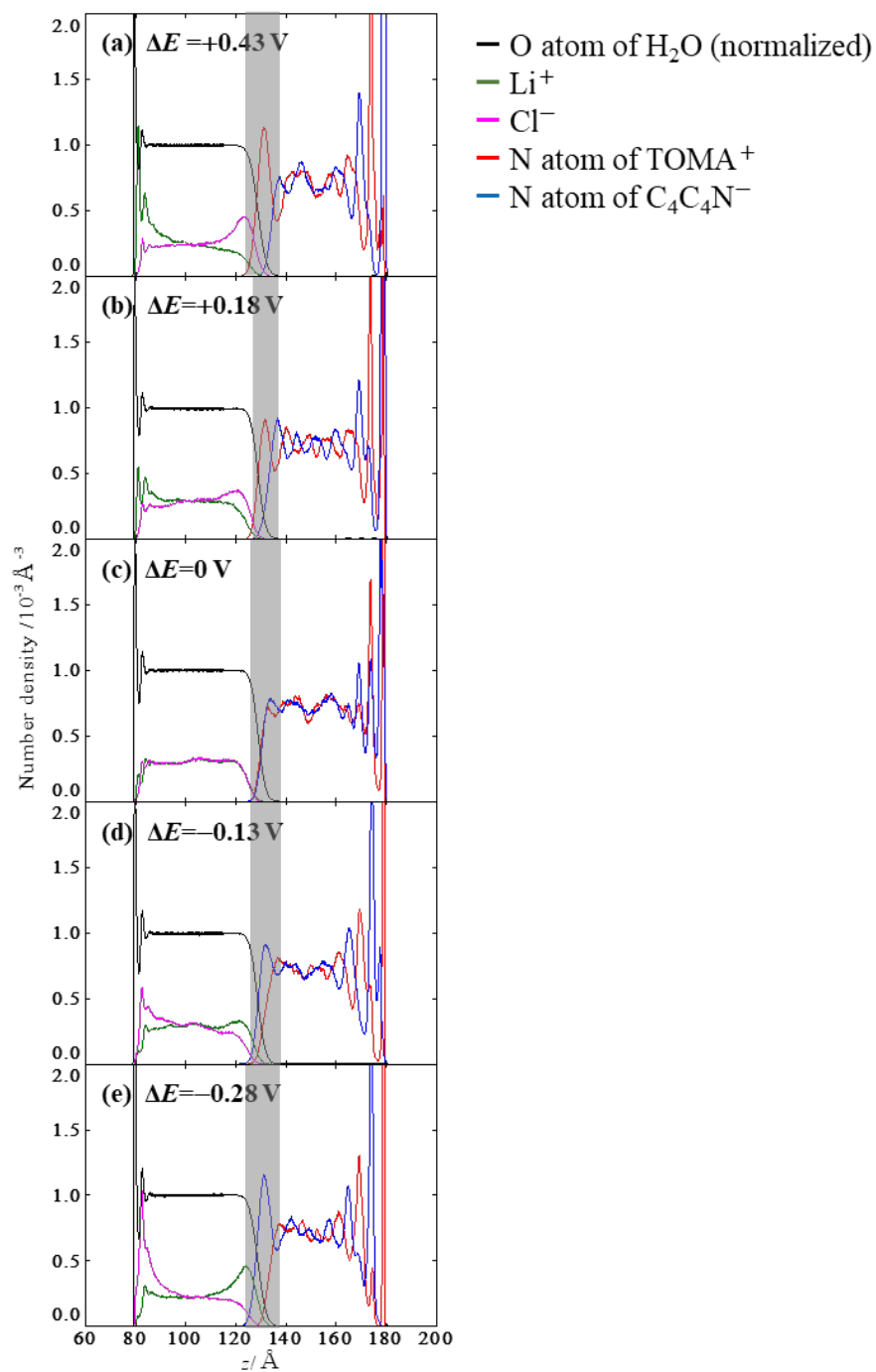


Fig.S4. Number density profiles for O atom of H_2O (black), N atom of TOMA^+ (red), N atom of $\text{C}_4\text{C}_4\text{N}^-$ (dark blue), Li^+ (dark green), and Cl^- (pink) at (a) $\Delta E = +0.43$, (b) $+0.18$, (c) 0 (d) -0.13 , and (e) -0.28 V. The profiles for the O atoms of H_2O are normalized to the bulk number density. The grey area indicates the interfacial first ionic layer where the orientations of IL ions were analyzed.

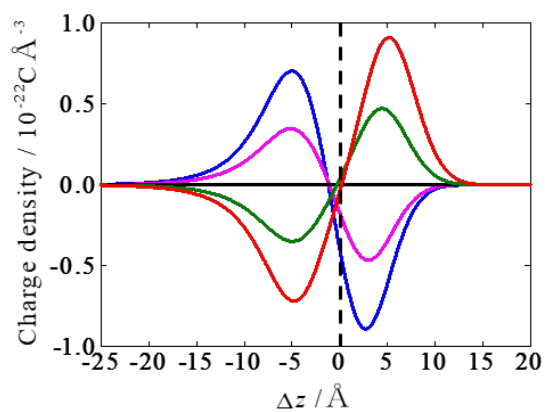


Fig.S5. Charge density distributions from the GCS-Oldham model at the IL|W interface at $\Delta E = +0.43$ (red), $+0.18$ (dark green), 0 (black), -0.13 (pink) and -0.28 V (blue). The thickness of the Stern layer on the W side was fixed to 3 \AA whereas that on the IL side was adjusted to be 3.9 , 3.6 , 2.0 , and 1.3 \AA for the four non-zero potentials ($\Delta E = +0.43$, $+0.18$, -0.13 , and -0.28 V, respectively) to reproduce the relationship between ΔE and σ_{IL} in MD. The vertical dotted line represents the position of the IL|W interface.

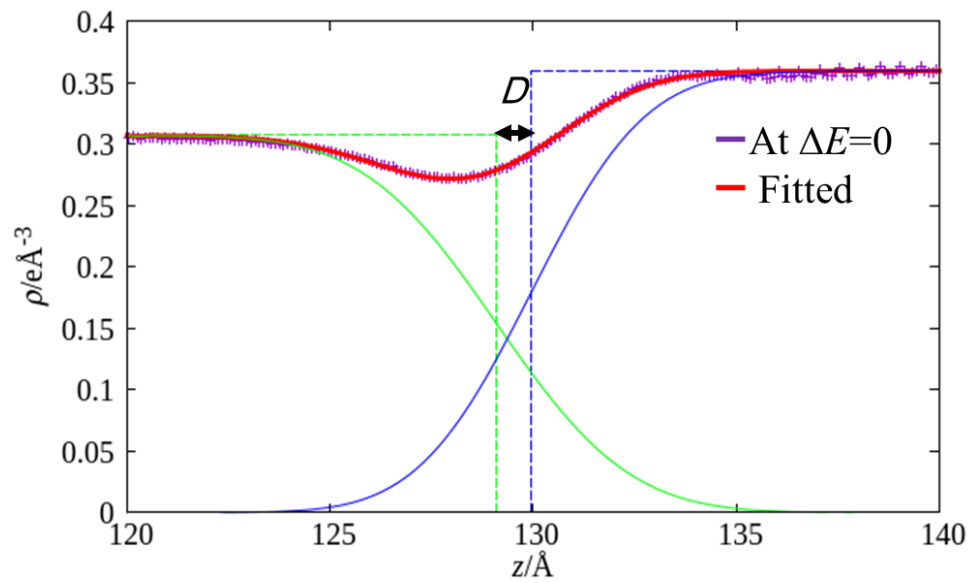


Fig.S6. Electron density distribution at $\Delta E=0$ (purple) and the fitted curve (red) with two error functions for W and IL (green and blue solid lines, respectively). The dashed green and blue lines are hypothetical error functions with zero width, showing the zero-density layer thickness D of 0.9 Å.

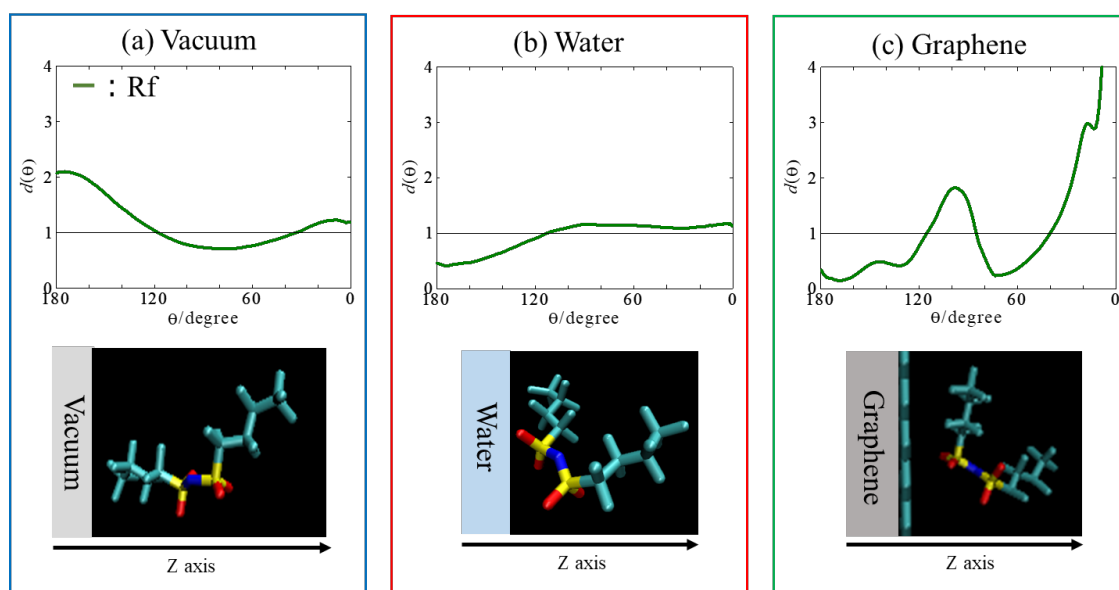


Fig.S7. Orientation distributions of $C_4C_4N^-$ at the (a) vacuum, (b) water, and (c) graphene interface of TOMAC $_4C_4N$ and snapshots showing typical orientations of $C_4C_4N^-$ at the interfaces.

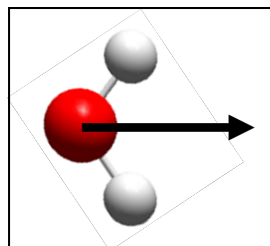


Fig.S8. Dipole moment vector of H₂O.

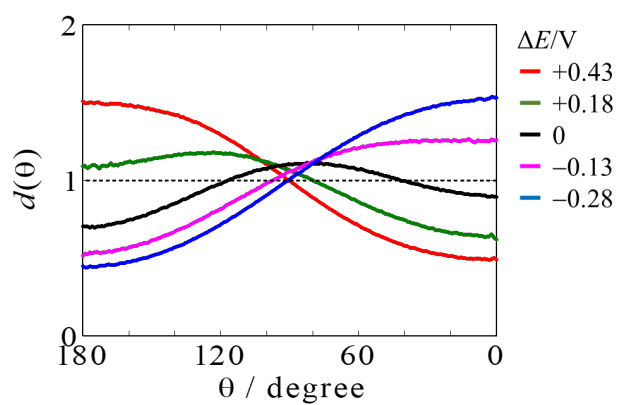


Fig.S9. Orientation distributions of the dipole moment of H₂O at $\Delta E = +0.43$ (red), $+0.18$ (green), 0 (black), -0.13 (pink), and -0.28 V (blue). The horizontal dotted line represents $d(\theta)=1$, an isotropic orientation. The z ranges analyzed are : 122-136 Å at $\Delta E = +0.43$ and -0.28 V; 123-135 Å at $\Delta E = +0.18$, -0.13 V; 125-134 Å at $\Delta E = 0$ V.

Table S1. Parameters of IL ions, Li^+ , and Cl^- . The van der Waals potential is described by Lennard-Jones potential, $4\epsilon\{(\sigma/r)^{12} - (\sigma/r)^6\}$.

atom name	atom type	mass / u	charge / e ^{a)}	σ / Å	ϵ / kJ mol ⁻¹
Nqa	NT	14.007	0.08490	3.25	0.71128
CM	CT	12.011	-0.12021	3.50	0.27614
CL1	CT	12.011	-0.12020	3.50	0.27614
CL2	CT	12.011	0.00710	3.50	0.27614
CL3	CT	12.011	-0.08485	3.50	0.27614
CL4	CT	12.011	-0.08485	3.50	0.27614
CL5	CT	12.011	-0.08485	3.50	0.27614
CL6	CT	12.011	-0.08490	3.50	0.27614
CL7	CT	12.011	-0.08490	3.50	0.27614
CL8	CT	12.011	-0.12727	3.50	0.27614
HM	HC	1.008	0.09190	2.50	0.12552
HL1	HC	1.008	0.09192	2.50	0.12552
HL2 to HL8	HC	1.008	0.04243	2.50	0.12552
NAA	NB	14.0000	-0.46700	3.25	0.71128
S	SB	32.066	0.72120	3.55	1.04600
O	OB	15.999	-0.37480	3.15	0.83736
CB1	CF	12.011	0.13435	3.50	0.27614
CB2	CF	12.011	0.16970	3.50	0.27614
CB3	CF	12.011	0.16970	3.50	0.27614
CB4	CF	12.011	0.25500	3.50	0.27614
FB1	FB	18.998	-0.11310	3.12	0.25540
FB2	F	18.998	-0.08485	2.95	0.22175
FB3	F	18.998	-0.08490	2.95	0.22175
FB4	F	18.998	-0.08490	2.95	0.22175
Li	Li	6.9410	1.00000	2.13	0.07648
Cl	Cl	35.453	-1.00000	3.65	0.83000

- a) Scaled by a factor of $\sqrt{2}$ from the original CL&P^{9,10} values to take into account the dielectric polarization (see SI text).

Table S2. Bond potential parameters of IL ions. The bond potential is described by harmonic oscillator potential, $(k_r/2)(r - r_0)^2$.

bond	r_0 / Å	k_r / kJmol ⁻¹
NT-CT	1.448	3196.6
CT-CT	1.529	2242.0
HC-CT	1.090	constraint
NB-SB	1.570	3137.0
SB-OB	1.437	5331.0
CF-SB	1.818	1950.0
CF-CF	1.529	2242.6
FB-CF	1.323	3698.0
F-CF	1.332	3071.1

Table S3. Angle potential parameters of IL ions. The angle potential is described by OPLS¹¹ potential, $(k_{\theta}/2)(r - r_0)^2$

angle	θ_0 / degree	k_{θ} / kJmol ⁻¹
SB-NB-SB	125.6	671.0
NB-SB-OB	113.6	789.0
NB-SB-OB	113.6	789.0
NB-SB-CF	103.5	764.0
OB-SB-OB	118.5	969.0
CF-SB-OB	102.6	870.0
NB-SB-OB	113.6	789.0
NB-SB-CF	103.5	764.0
SB-CF-CF	115.9	418.4
FB-CF-SB	111.7	694.0
FB-CF-CF	109.5	418.4
CF-CF-CF	112.7	488.3
F-CF-CF	109.5	418.4
F-CF-F	109.1	644.3

Table S4. Dihedral potential parameters of IL ions. The Dihedral potential is described by OPLS¹¹ potential, $\sum_{m=1}^4 (V_m/2)[1 + (-1)^{m+1}\cos(m\varphi)]$.

dihedral	V1 / kJmol ⁻¹	V2 / kJmol ⁻¹	V3 / kJmol ⁻¹	V4 / kJmol ⁻¹
HC-CT-CT-NT	-4.2384	-2.9665	1.9790	0.0000
HC-CT-NT-CT	0.0000	0.0000	2.3430	0.0000
CT-CT-CT-NT	10.0081	-2.8200	2.3012	0.0000
CT-NT-CT-CT	1.7405	-0.5356	2.9079	0.0000
HC-CT-CT-HC	0.0000	0.0000	1.2552	0.0000
CT-CT-CT-HC	0.0000	0.0000	1.2552	0.0000
CT-CT-CT-CT	5.4392	-0.2092	0.8368	0.0000
OB-SB-NB-SB	0.0000	0.0000	-0.0150	0.0000
SB-NB-SB-CF	32.7730	-10.4200	-3.1950	0.0000
NB-SB-CF-CF	-3.0940	0.0000	0.0000	0.0000
OB-SB-CF-CF	0.0000	0.0000	-0.7400	0.0000
NB-SB-CF-FB	0.0000	0.0000	1.3220	0.0000
OB-SB-CF-FB	0.0000	0.0000	1.4510	0.0000
SB-CF-CF-CF	50.0900	0.0000	-4.6260	-4.0080
FB-CF-CF-CF	1.2552	0.0000	1.6736	0.0000
F-CF-CF-FB	-10.4600	0.0000	1.0460	0.0000
SB-CF-CF-F	0.0000	0.0000	1.4530	0.0000
CF-CF-CF-CF	27.7064	3.9664	-5.8074	-8.8617
F-CF-CF-CF	1.2552	0.0000	1.6736	0.0000
F-CF-CF-F	-10.4600	0.0000	1.0460	0.0000

References

- 1 <https://github.com/paduagroup/fftool> (2020).
- 2 L. Martínez, R. Andrade, E. G. Birgin and J. M. Martínez, *J. Comput. Chem.*, 2009, **30**, 2157–2164.
- 3 H. J. C. Berendsen, J. P. M. Postma, W. F. Van Gunsteren, A. Dinola and J. R. Haak, *J. Chem. Phys.*, 1984, **81**, 3684–3690.
- 4 S. Nosé, *Mol. Phys.*, 1984, **52**, 255–268.
- 5 W. G. Hoover, *Phys. Rev. A*, 1985, **31**, 1695–1697.
- 6 S. Katakura, N. Nishi, K. Kobayashi, K. I. Amano and T. Sakka, *J. Phys. Chem. C*, 2019, **123**, 7246–7258.
- 7 L. F. Scatena, M. G. Brown and G. L. Richmond, *Science*, 2001, **292**, 908–912.
- 8 D. S. Walker, F. G. Moore and G. L. Richmond, *J. Phys. Chem. C*, 2007, **111**, 6103–6112.
- 9 J. N. Canongia Lopes and A. A. H. Pádua, *Theor. Chem. Acc.*, 2012, **131**, 1129.
- 10 A. S. L. Gouveia, C. E. S. Bernardes, L. C. Tomé, E. I. Lozinskaya, Y. S. Vygodskii, A. S. Shaplov, J. N. Canongia Lopes and I. M. Marrucho, *Phys. Chem. Chem. Phys.*, 2017, **19**, 29617–29624.
- 11 R. C. Rizzo and W. L. Jorgensen, *J. Am. Chem. Soc.*, 1999, **121**, 4827–4836.